Modeling the Size Distribution and Chemical Composition of Secondary Organic Aerosols during the Reactive Uptake of Isoprene-Derived Epoxydiols under Low-Humidity Condition

Mega Octaviani, Manish Shrivastava,* Rahul A. Zaveri, Alla Zelenyuk, Yue Zhang, Quazi Z. Rasool, David M. Bell, Matthieu Riva, Marianne Glasius, and Jason D. Surratt

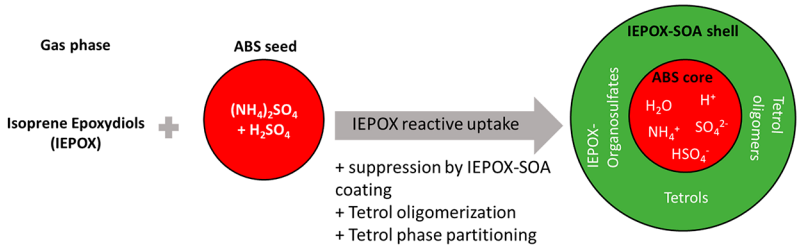

ABSTRACT: Reactive uptake of isoprene epoxydiols (IEPOX), which are isoprene oxidation products, onto acidic sulfate aerosols is recognized to be an important mechanism for the formation of isoprene derived secondary organic aerosol (SOA). While a mechanistic understanding of IEPOX SOA formation exists, several processes affecting their formation remain uncertain. Evaluating mechanistic IEPOX SOA models with controlled laboratory experiments under longer atmospherically relevant time scales is critical. Here, we implement our latest understanding of IEPOX SOA formation within a box model to simulate the measured reactive uptake of IEPOX on polydisperse ammonium bisulfate seed aerosols within an environmental Teflon chamber. The model is evaluated with single particle measurements of size distribution, volume, density, and composition of aerosols due to IEPOX SOA formation at time scales of hours. We find that the model can simulate the growth of particles due to IEPOX multiphase chemistry, as reflected in increases of the mean particle size and volume concentrations, and a shift of the number size distribution to larger sizes. The model also predicts the observed evolution of particle number mean diameter and total volume concentrations at the end of the experiment. We show that in addition to the self limiting effects of IEPOX SOA coatings, the mass accommodation coefficient of IEPOX and accounting for the molar balance between inorganic and organic sulfate are important parameters governing the modeling of the IEPOX SOA formation. Thus, models which do not account for the molar sulfate balance and/or diffusion limitations within IEPOX SOA coatings are likely to predict IEPOX SOA formation too high.

KEYWORDS: *secondary organic aerosols, isoprene epoxydiols, multiphase chemistry, chamber measurements, box modeling, size distribution, chemical composition, low relative humidity*

INTRODUCTION

Isoprene (2 methyl 1,3 butadiene) is the nonmethane volatile organic compound (VOC) emitted in the largest amount to the atmosphere, with an estimated annual global emission from vegetation of 440−660 tera grams of carbon (TgC).[1] Its abundance and rapid oxidation by hydroxyl (OH) radicals (k = 9.7 × 10^{-11} cm^3 $molec^{-1}$ s^{-1})[2] plays a crucial role in tropospheric chemistry, particularly throughout forested regions in tropical and midlatitude areas. Isoprene oxidation products are significant contributors to the global budget of secondary organic aerosols (SOA),[3−5] and influence the growth and evolution of particles in ambient air, as demonstrated during laboratory experiments[6−12] and field studies[13−16] under low and high concentrations of nitrogen oxide (NO_x = NO + NO_2) conditions. On a global scale, the latest estimate of a net SOA production rate from oxidation of isoprene and other biogenic VOC is between 10 and 150 TgC yr^{-1}, contributing to at least 25% of total organic aerosol mass.[17,18]

Under low NO_x conditions, OH initiated isoprene oxidation followed by subsequent reaction of isoprene peroxy radicals with hydroperoxyl (HO_2) radicals leads to the formation of isoprene hydroxyhydroperoxide (ISOPOOH) in yields exceed

ing 70%.[19,20] ISOPOOH reacts further by OH radical addition and isomerization to form isoprene epoxydiols (IEPOX), with yields exceeding 75%.[20] Subsequent multiphase chemistry of IEPOX in the presence of aqueous, acidified sulfate aerosols has been shown to be a major source of isoprene derived SOA mass.[10,21,22] IEPOX uptake into the aerosol phase with further transformation via a ring opening mechanism and nucleophilic addition in aqueous particles[22−24] explains the formation of known isoprene SOA products found in ambient aerosols, namely 2 methyltetrols, IEPOX derived organosulfates (OSs), and oligomeric species.[10,22,25] Recent field measurements have demonstrated the importance of IEPOX derived SOA products in fine organic aerosols.[26−31] In certain regions of the southeastern US, IEPOX SOA tracers represent up to one third of the total fine organic aerosol mass during the summer, with 2 methyltetrols and IEPOX organosulfates contributing up to 33−47% and 15−34% of the total IEPOX SOA, respectively.[27,28,31]

The reactive uptake of gas phase IEPOX to atmospheric particles is represented by an uptake coefficient (γ_{IEPOX}). Laboratory measurements of the IEPOX uptake onto aerosol particles confirmed an increase in γ_{IEPOX} with increasing aerosol acidity.[32,33] Furthermore, relative humidity (RH) and the presence of organic coatings also play a role in IEPOX uptake.[32,34−37] For pure sulfate seed particles, γ_{IEPOX} exhibits an inverse correlation with RH wherein higher humidity impedes further IEPOX uptake as aerosol particles take up more water since their acidity and ionic concentrations decrease.[32,34] Further insights into the morphology of the internally mixed organic/inorganic particles show that the presence of pre existing SOA coatings on sulfate particles would undergo liquid−liquid or semisolid−liquid phase separation into an organic rich shell surrounding a sulfate containing aerosol core.[36−38] The organic shell (or coating) can suppress the acid catalyzed heterogeneous reactions of IEPOX, as demonstrated in previous laboratory studies,[32,34,35] and reduce γ_{IEPOX} substantially, especially at lower RH conditions wherein OA viscosity and bulk diffusion limitations are higher.[34] In addition, IEPOX SOA formation self limits further IEPOX uptake. A recent study confirms that IEPOX SOA components 2 methyltetrols and organosulfates are highly viscous and cause strong particle phase diffusion limitations as they form a coating around the inorganic seeds during their formation.[39,40]

Prior IEPOX SOA modeling studies have used a resistor based parameterization, using constraints on IEPOX solubility and reactivity, as described in Anttila et al.[41] and Gaston et al.[42] The reactivity of IEPOX is represented by an overall particle phase reaction rate constant, in which the rate determining step depends on which of the two distinct reaction pathways, known as A 1 and A 2 mechanism, is taken.[24] Kinetic studies using bulk solutions have provided estimates of the epoxide reaction rate constants for a variety of acid catalyzed ring opening reactions.[24,43−45] Several regional/global models have implemented the γ_{IEPOX} resistor based model for aqueous IEPOX SOA formation and found improved model predictions of SOA mass yield when compared to field observations.[37,46−48]

Previous studies (e.g., Gaston et al.[32]) have measured the loss rate of IEPOX gas due to its reactive uptake on acidic sulfate particles in a flow tube at short time scales (~10−20 s) and have shown that the resistor based model can explain the IEPOX gas loss kinetics. However, to the best of our knowledge, the resistor model formulation has not been tested against direct measurements of particle size evolution due to IEPOX SOA formation, especially at longer time scales on the order of hours in environmental chambers. Recently, such single particle measurements have been conducted character izing how IEPOX uptake on acidic sulfate particles in a Teflon chamber affects particle size, composition, and density evolution,[35] providing a unique opportunity to understand IEPOX SOA processes through application of this modeling framework.

In this study, we integrated and applied new IEPOX SOA modeling capabilities in a box model to understand kinetic processes governing evolution of particle size, chemical composition, and overall particle density due to reactive uptake of IEPOX, as measured by Riva et al.[35] The capability of a chemistry aerosol inorganic box model, Model for Simulating Aerosols Interaction and Chemistry (MOSAIC), developed by Zaveri et al.,[49] was extended to include key processes of IEPOX SOA formation on polydisperse aerosols. The MOSAIC model is also widely used in regional and global chemical transport models, that is, the Weather, Research and Forecasting model with Chemistry (WRF Chem)[50,51] and the Community Earth System Model (CESM).[52] We then applied the model to predict the particle size evolution and SOA composition upon IEPOX uptake by pure ammonium bisulfate particles from the chamber experiments reported in Riva et al.[35] This work focuses on a single aerosol system, ammonium bisulfate seed aerosols under dry conditions (<5% RH).

METHODS

MOSAIC Model. In this study, we added IEPOX reactive uptake parameterizations on ammonium bisulfate (ABS) seed aerosols to the sectional aerosol box model MOSAIC.[49,53] The model treats gas and aerosol chemistry, aerosol thermody namics and phase state, aerosol microphysical processes such as coagulation and condensation, and particle wall loss. At every time step, it dynamically partitions nonvolatile and semivolatile organic and inorganic gases to size resolved particles and predicts particle phase water and pH (acidity) in each size bin. Gas−particle mass transfer calculation takes into account compound volatility, gas phase diffusion, interfacial accommodation, and particle phase bulk diffusion in the semisolid organic phase. For this study, particle size distribution was represented using the moving bin approach wherein coagulation was ignored, since effects of coagulation were found to be insignificant. MOSAIC was updated as described in the Methods to simulate the multiphase chemistry, formation, and time evolution of IEPOX SOA and the resulting changes in particle size distributions and compositions within an environmental Teflon chamber.

Chamber Measurements. We used the results from the experimental chamber study described by Riva et al.[35] to initialize the model with measured IEPOX gas, particle size distributions, and seed composition, and to evaluate model parameters related to IEPOX SOA formation. Briefly, their experiments were conducted in a 1 m^3 Teflon chamber under dry (<5% RH) conditions at room temperature (24 ± 2 °C) and atmospheric pressure (1 atm). Acidified ammonium sulfate (ammonium bisulfate, ABS) seed aerosols were generated by nebulizing aqueous solutions of 0.06 M $(NH_4)_2SO_4$ (aq) + 0.06 M H_2SO_4 (aq). The ABS seed particles were then introduced into the chamber before the injection of 500 ppb *trans β* IEPOX, the proposed dominant

IEPOX isomer mixture.[19] *trans β* IEPOX was synthesized in high purity (>99%) by the UNC group following published procedures.[54] A 2.5 mg sample of trans *β* IEPOX was introduced into the chamber and mixed with the ABS seed particles by passing high purity N_2 gas at 2 L min^{-1} through a heated manifold (60−70 °C) for 30 min.[35] A scanning mobility particle sizer (SMPS), which consists of a differential mobility analyzer (DMA) and a condensation particle counter (CPC), was used to periodically measure the size distributions of particle number, surface area, and volume concentrations during the IEPOX uptake into the ABS seed aerosols. The single particle mass spectrometer (miniSPLAT)[55] was used to perform online in situ measurements of size, density, shape, and chemical composition of individual particles inside the chamber at a time resolution of a few minutes. A schematic of the chamber employed is shown in Figure S1. At the end of each experiment, particles were collected onto Teflon membrane filters for offline analysis of IEPOX derived SOA bulk chemical composition using ultraperformance liquid chromatography/electrospray ionization, high resolution quad rupole time of flight mass spectrometry (UPLC/ESI QTOFMS), and gas chromatography/electron ionization mass spectrometry (GC/EI MS). The experiments were also performed using deliquesced ammonium sulfate seed particles and ABS coated with SOA produced from *α* pinene ozonolysis to investigate the effect of acidity and organic coating on IEPOX uptake. Further experimental details are provided in Riva et al.[35] The present study focuses on modeling IEPOX uptake onto ABS seeds under dry conditions (i.e., < 5% RH). ABS particles, even at very low RHs, are not crystalline and instead exist in metastable states that contain some particle water,[56] which explains their high acidity and high reactivity with IEPOX under dry conditions.

IEPOX Reactive Uptake. The heterogeneous reactive uptake of gas phase IEPOX on acidic seed particles is defined in terms of first order kinetics:

$$\frac{d[IEPOX_g]}{dt} = -\frac{\gamma_{IEPOX}}{4} A_p \langle c \rangle [IEPOX_g] \quad (1)$$

where A_p is the particle surface area ($cm^2\ cm^{-3}$), $[IEPOX_g]$ is the gas phase IEPOX concentration (mol m^{-3}), and $\langle c \rangle$ is the mean molecular speed (cm s^{-1}). The reactive uptake coefficient of IEPOX (γ_{IEPOX}) is calculated following a resistor model described in Anttila et al.[41] that includes possible mass transfer limitations caused by organic coatings:

$$\frac{1}{\gamma_{IEPOX}} = \frac{\langle c \rangle r_p}{4D_{gas}} + \frac{1}{\alpha} + \frac{\langle c \rangle r_p}{4RTH_{org}D_{org}(q_{org}F - 1)} \quad (2)$$

where D_{gas} is the gas phase diffusion coefficient ($cm^2\ s^{-1}$) which is estimated as $D_{gas} = 1.9\ MW^{-2/3}$ with MW being the molecular weight of IEPOX (118 g mol^{-1}), α is the mass accommodation coefficient of IEPOX (0.02 or 0.1 used here based on previous studies[32,46,57]), R is the ideal gas constant (L atm K^{-1} mol^{-1}), and T is the temperature (K). H_{org} and D_{org} are the Henry's law constant and diffusion coefficient of the reactant (IEPOX or 2 methyltetrols in the gas phase) in the organic coating, respectively. The terms H_{org} and D_{org} were assumed to be independent of particle size. The $H_{org}D_{org}$ value was determined based on SOA viscosity measurements generated from a flow tube reactor conducted under a RH range of 40−99% with an extrapolation for RH < 40% (Figure S2).[34] We selected the $H_{org}D_{org}$ value at 35% RH for the current study (i.e., 6.34×10^{-8} M atm^{-1} $cm^2\ s^{-1}$), as opposed to the value at the simulated dry condition of <5% RH. Using extrapolated $H_{org}D_{org}$ values below 35% RH completely shut off the reactive uptake of IEPOX (see Figure S3) and was inconsistent with observed particle growth measurements in Riva et al.[35] and other experiments at low RH.[32,34] H_{org} was set to 2.0×10^6 M atm^{-1}, as used in Zhang et al.,[34] resulting in 3.16×10^{-14} $cm^2\ s^{-1}$ for D_{org}.

The function F is a composite term for processes involved in the reactive uptake at the interface between two bulk phases and is expressed as

$$F = \frac{\coth(q_{org}) + h(q_{aq}, q^*_{org})}{1 + \coth(q_{org})h(q_{aq}, q^*_{org})} \quad (3)$$

$$h(q_{aq}, q^*_{org}) = -\tanh(q^*_{org}) \left[\frac{\frac{H_{aq}D_{aq}}{H_{org}D_{org}}(q_{aq}\coth(q_{aq}) - 1) - (q^*_{org}\coth(q^*_{org}) - 1)}{\frac{H_{aq}D_{aq}}{H_{org}D_{org}}(q_{aq}\coth(q_{aq}) - 1) - (q^*_{org}\tanh(q^*_{org}) - 1)} \right] \quad (4)$$

$$q^*_{org} = \frac{r_c}{r_p} q_{org} \quad (5)$$

$$q_{aq} = r_c\sqrt{\frac{k_{aq}}{D_{aq}}}, \qquad q_{org} = r_p\sqrt{\frac{k_{org}}{D_{org}}} \quad (6)$$

Here, H_{aq} and D_{aq} are the Henry's laws constant (3.0×10^7 M atm^{-1}) and diffusion coefficient (1.0×10^{-5} $cm^2\ s^{-1}$) of the reactant in the inorganic aqueous core, respectively. The parameters q_{aq} and q_{org} are diffuso reactive parameters that describe the competition between diffusion and reaction in the aqueous core and organic coating, respectively. The parameters are defined as a function of their diffusion coefficients (D_{aq} and D_{org}), radius of inorganic aqueous core (r_c) and overall particle radius (r_p = r_c + organic coating thickness) in cm, and the first order reaction rate constants (k_{aq} and k_{org}) in s^{-1}. We performed a sensitivity study on model results to H_{aq} as this parameter is known to vary by several orders of magni tude.[32,47,57] Figure S4 shows that increasing H_{aq} directly contributes to an increase in SOA mass and aerosol growth, but the rate starts to slow down and the model becomes less sensitive to H_{aq} when it is higher than our default value, which is derived from measurements[44] and has been applied in past modeling studies.[28,57−59]

The above set of eqs 1−6 simulate IEPOX uptake into internally mixed organic/inorganic particles using ABS as the inorganic core and IEPOX SOA as the organic shell. Measurements show that ABS is a highly hygroscopic substance that does not effloresce even around 0% RH and exists in a deeply metastable phase.[56] Consistent with these measurements, we assumed that ABS particles remain in a metastable liquid state at 5% RH in our MOSAIC model formulation, and its water content and acidity were approximated by not allowing the particles to effloresce.

A recent laboratory study by Zhang et al.[39] examined the implications of IEPOX SOA on the reactivity of pre existing sulfate particles. They found that aerosol acidity decreases, and viscosity increases after IEPOX reactive uptake, leading to a self limiting effect in which newly formed IEPOX derived SOA inhibits additional multiphase chemical reactions of IEPOX.

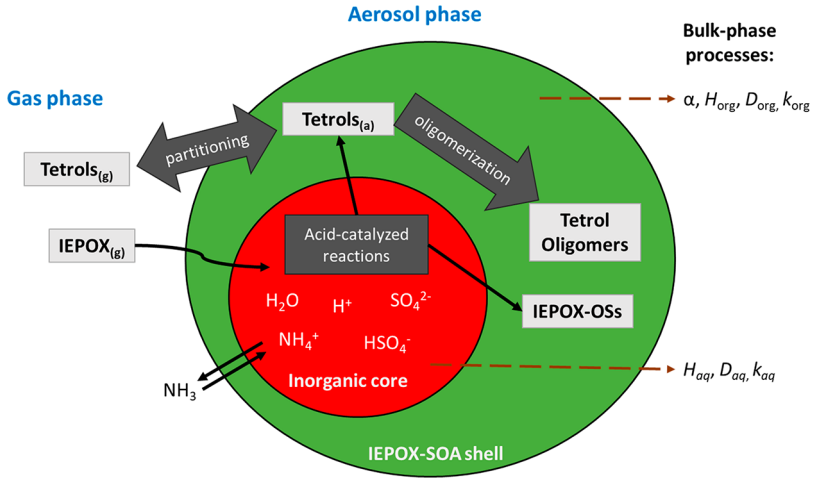

Figure 1. Schematic of IEPOX SOA multiphase chemistry and gas−particle partitioning processes represented in the box model.

To account for this finding, we impose a molar balance between inorganic sulfate and organosulfates (part of IEPOX SOA), that is, as organosulfate forms, an equimolar amount is lost from inorganic sulfate at each model time step.

We applied a one second time step to simulate the 2 h chamber experiment. The number of size bins was set to 205, with the diameters of upper and lower boundaries being 1.08 and 1715.45 nm, respectively. The model was initialized with gaseous IEPOX of 500 ppb and the SMPS measured seed aerosol size distribution before the IEPOX injection. In the study, the density of 1.5 g cm^{-3} was assumed for each SOA tracer (2 methyltetrols, OSs, and oligomers), which follows an estimate applied in Cui et al.[60] It is noted that based on the miniSPLAT measurements, the density of ABS particles under dry conditions is 1.77 g cm^{-3}, while the final aerosol density after reaction with IEPOX is 1.48 g cm^{-3}. Molecular weights (MW) of 136, 216, and 250 g mol^{-1} were assigned for 2 methyltetrols, OSs, and oligomers, respectively. Oligomers of tetrols were assumed to be similar to a hemiacetal dimer of 2 IEPOX molecules, which has a MW of ∼254 g mol^{-1}.[10,14] The aerosol mass and number concentrations were assumed to be continuously and irreversibly lost to the walls of the Teflon chamber with a first order rate determined by fitting the measured loss in total particle number concentrations over the entire experiment (see section S 1d in the Supporting Information). Gas phase wall losses were neglected, implicitly assuming that gases deposited on the chamber walls were available to interact with particles suspended in the chamber. A sensitivity simulation where gas phase absorption and desorption from the chamber walls was included, produced similar particle size evolution as when gas phase wall losses were turned off (not shown).

Aqueous-Phase Reaction Rate Constant. The aqueous phase reaction rate constant (k_{aq}) for IEPOX is calculated assuming protonation of IEPOX and nucleophilic addition following the A 2 mechanism of Eddingsaas et al.[24] We thus implemented the following definition of k_{aq}:[43,46,47]

$$k_{aq} = \sum_{i=1}^{N} \sum_{j=1}^{M} k_{i,j}[\text{acid}_i][\text{nuc}_j] \tag{7}$$

This expression implies that the overall rate of reaction is determined by the third order rate constants ($k_{i,j}$, in M^{-2} s^{-1}) multiplied by the concentrations (mol L^{-1} within particle phase) of acids (H^+, HSO_4^-, NH_4^+) and nucleophiles (H_2O and SO_4^{2-}) in the model. IEPOX uptake by aerosols forms two major SOA products, namely 2 methyltetrols (tetrols) and IEPOX organosulfates (i.e., methyltetrol sulfates or OSs), based on a previous study.[61] The fraction of IEPOX SOA attributed to OS (β) was determined based on the relative contribution of the OS formation rate to the effective first order rate constant. The experimental values of $k_{i,j}$ were adopted from different kinetic studies compiled in Budisulistiorini et al.[46] and summarized in the Supporting Information (Section S1b and Table S1).

Tetrol Phase Partitioning and Oligomerization. While OSs were assumed to be fully nonvolatile (consistent with the measurements of evaporation kinetics of OS standards), tetrols were treated as semivolatile which means some fraction of tetrols will partition out of the aerosols depending on the organic mass loadings. However, particle phase tetrols were also assumed to form nonvolatile oligomers at a first order time scale of ∼2 h, which reduces their evaporation/partitioning to the gas phase, as discussed later. We assumed the saturation vapor concentration (C^*) of 10 μg m^{-3} for tetrols based on the range of C^* estimates of 5−15 μg m^{-3} reported in an environmental chamber study.[61] The mass accommodation coefficient (α) of 0.1 for tetrols was applied. Diffusion limitations to the partitioning were treated based on Zaveri et al.,[53] with the particle bulk diffusivity of 3.16×10^{-14} cm^2 s^{-1} (to be consistent with the D_{org} parameter in eq 2). We also assumed that particle phase tetrols undergo oligomerization to form nonvolatile tetrol oligomers (hereinafter, referred to as oligomers) with a first order e folding time scale (τ_{olig}) of 2 h based on measurements reported in D'Ambro et al.[61] that the low volatility mode of $C_5H_{12}O_4$ desorption (similar in structure to 2 methyltetrols) was formed quickly via acid enhanced accretion chemistry within a few hours. To be consistent with the oligomerization time scale of 2 h (7200 s), k_{org} in eq 6 was assumed to be a constant, that is, 1/7200 s^{-1}. We found that the reactive uptake coefficient of IEPOX (γ_{IEPOX}, eq 2) is not as sensitive to the k_{org} value except when k_{org} is very fast (10 s^{-1}), that is, a time scale of 0.1 s (instead of 2 h) or faster.

IEPOX-SOA Processes. Figure 1 schematically illustrates the key multiphase chemical processes during reactive uptake of IEPOX gas on aqueous acidic sulfate seed aerosols, dynamic gas particle partitioning of tetrols and their oligomerization.

Table 1. Model Setup and Summary of Observed and Simulated Results

observations/ simulation	inorganic sulfate removal	IEPOX accommodation coeff	final mean diameter (nm)	final total vol concn (μm^3 cm^{-3})	IEPOX-SOA nonvolatile fraction (%)
Observations			127.5	42.3	90.0
Base	on	0.02	118.8	32.5	94.0
HighAccom	on	0.1	128.4	37.3	93.3
KeepSO4	off	0.02	189.6	79.8	87.8

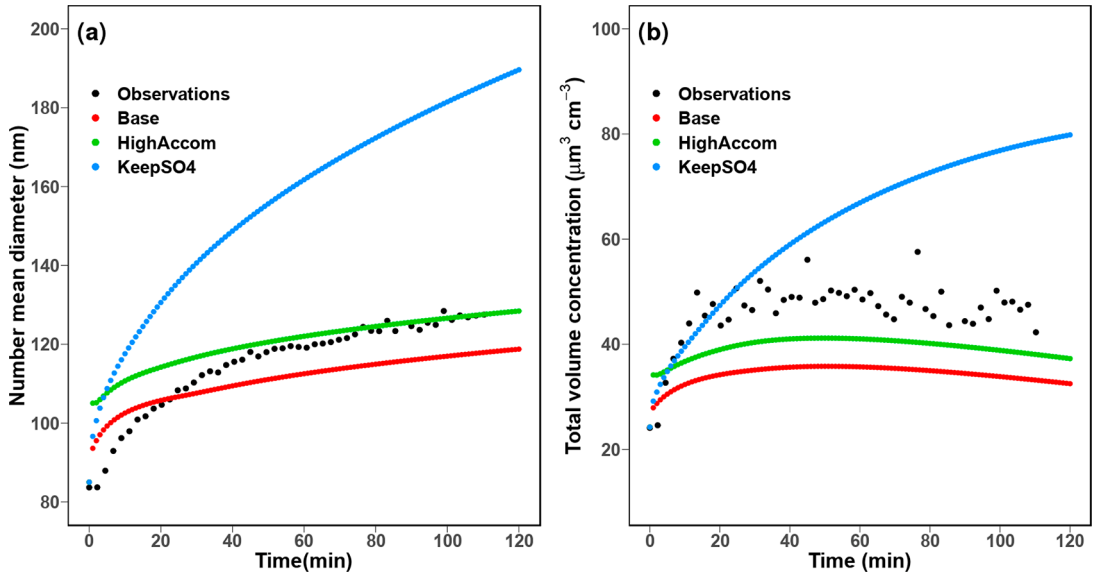

Figure 2. Time evolution of (a) aerosol number mean diameter (nm) and (b) total suspended aerosol volume concentrations (μm^3 cm^{-3}) from observations (black dots) and all model simulations (color lines).

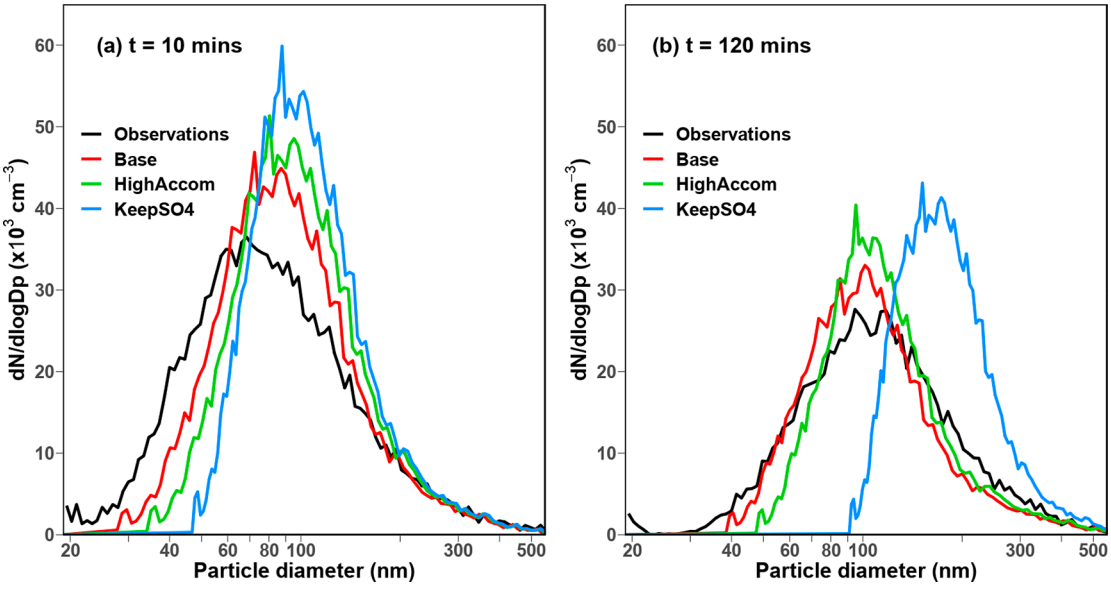

Figure 3. Size distributions of aerosol number concentrations from observations (black lines) and all model simulations (color lines) at (a) 10 and (b) 120 min after the introduction of IEPOX gas onto ammonium bisulfate aerosols in a 1 m^3 chamber.

After IEPOX gas dissolves in aqueous sulfate seed particles due to its high water solubility, it undergoes an acid catalyzed particle phase conversion to form tetrols and OSs. Tetrols are semivolatile and can partition back to the gas phase, but our simulations indicate that ~50% of the tetrols are converted to nonvolatile oligomers at an e folding time scale of 2 h. Formation of OSs consumes inorganic sulfate, decreasing particle acidity, density, and hygroscopicity.[11,35,39] IEPOX SOA also forms a shell around the inorganic core, and as more IEPOX SOA forms, it limits further uptake of IEPOX gases.[11] We simulated these complex processes in a box model and evaluated how these processes affect size distribution, chemical composition, and density of the particles with respect to single particle measurements. This multiparameter model evaluation provides unique insights and significant advances in our understanding of IEPOX SOA formation.

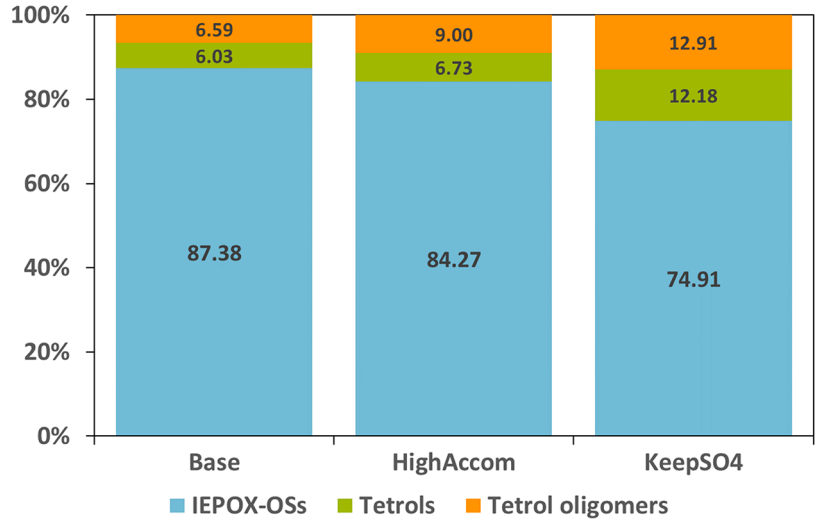

Figure 4. Relative contributions (% by mass, labels indicate the percentage values) of simulated IEPOX derived SOA tracers for each scenario after 2 h: IEPOX organosulfate (OS), 2 methyltetrols (Tetrols), and tetrol oligomers.

We further performed two sensitivity tests to examine how mass accommodation coefficient and inorganic to organic sulfate conversion affect model performance compared to our default (base case) scenario (Table 1).

RESULTS AND DISCUSSION

Base Case Scenario. Following IEPOX uptake and SOA formation, measurements show that the particle number mean diameter increases by 52% and total suspended particle volume increases by a factor of 2 over 2 h, reaching final values of 127.5 nm and 42.3 μm^3 cm^{-3}, respectively (black solid markers in Figure 2). Note that actual increase in particle volume due to IEPOX SOA formation is larger if we account for particles lost to the walls of the chamber. In the base case scenario, the model is able to reproduce the observed mean diameter and volume evolution, but moderately underestimates their magnitudes by an average 5% and 25%, respectively (red solid line in Figure 2). At the end of the simulation, the model predicted mean diameter is 118.8 nm and the total volume is 32.5 μm^3 cm^{-3} (Table 1).

Figure 3 shows the evolution of particle number size distributions ($dN/dlogD_p$). The observed particle size distributions are unimodal and dominated by particles in the range of 50−90 nm after 10 min and ∼80−150 nm after 2 h. The base case model well reproduces the observed characteristics of the unimodal structure with a shift to larger sizes as particles grow with IEPOX SOA formation. The model overestimates the initial growth of particles during the first 10 min as compared to the observations. These differences most likely relate to the fact that the model was initialized "instantaneously" with gaseous IEPOX of 500 ppb and the SMPS measured seed aerosol size distribution before the IEPOX injection, whereas in the experiment, it took a few minutes to inject IEPOX into the 1 m^3 chamber and mix it with the ABS seed particles. Figure 2a indicates that the model reaches half of its maximum growth only within ∼10 min, opposed to ∼15 min as seen in observations[35] but reproduces the final size distribution at the end of the experiment (2 h) (Figure 3b).

Figure 4 shows that OSs are predicted to heavily dominate IEPOX SOA constituents (87.4%), followed by tetrols (6.0%) and tetrol oligomers (6.6%). Filter analysis by GC/EI MS and UPLC/ESI QTOFMS reports that 2 methyltetrols and IEPOX derived OSs contribute to approximately 10% and 50−60% of IEPOX SOA tracers, respectively (as shown in Figure 2 of Riva et al.[35]). The observations show that these species have important contributions to total SOA mass (∼40%), consistent with previous studies that analyzed ambient $PM_{2.5}$ samples.[22,27] C5 alkene triols are not explicitly predicted from the model, but some studies reported that these could be thermal decomposition products of 2 methyltetrol sulfates.[60,61] As demonstrated in Cui et al.,[60] during GC−MS measurements, IEPOX derived OSs can decompose into C5 alkene triols (analytical GC−MS measurement artifacts) and to a smaller extent to 2 methyltetrols. Therefore, the sum of measured IEPOX OS (and their dimers/trimers) and C5 alkene triols accounting for ∼90% of IEPOX SOA in Figure 2 of Riva et al.[35] can be compared to our predictions of OS. Since simulated OS represents 87% of IEPOX SOA, these are in good agreement with the sum of IEPOX OS and C5 alkene triols in Riva et al.[35] Given the analytical artifacts involved in characterizations of IEPOX SOA components especially through techniques involving thermal decomposition, evaluating the simulated total nonvolatile content of IEPOX SOA with observations is a key part of this puzzle. Our simulations show that the nonvolatile content of IEPOX SOA is 94% (sum of OSs and tetrol oligomers; Table 1). Complementary measurements of IEPOX SOA evaporation kinetics at room temperature show that ∼90% of IEPOX SOA is nonvolatile (Table 1). Thus, the simulated IEPOX SOA nonvolatile content agrees with measurements, which is encouraging given that particle volatility drives its lifetimes in the atmosphere.

Another important evaluation metric is total particle density, since overall density depends on particle chemical composition. The overall density of particles (organic + inorganic) measured by miniSPLAT is reported to be 1.48 ± 0.02 g cm^{-3}.[35] Our model predicted final particle density achieves acceptable agreement with these measurements and predicts aerosol density slightly increasing with particle size ranging between 1.50 and 1.65 g cm^{-3} (Figure S6), indicating less than 12% difference between model and observations. The higher

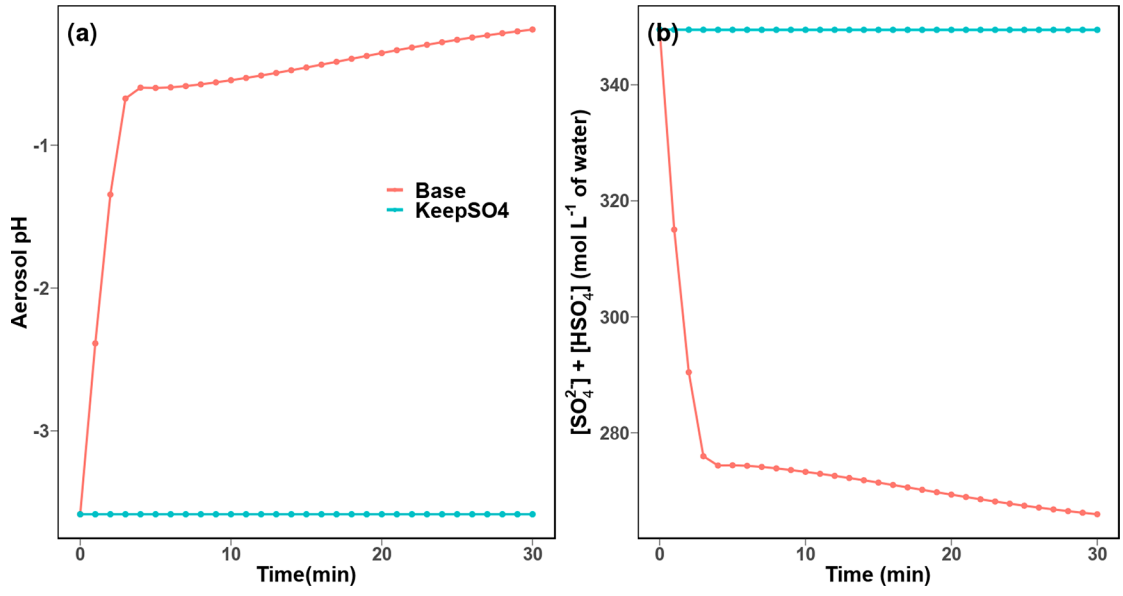

Figure 5. Time evolution of (a) simulated aerosol pH and (b) total sulfate concentration (mol L^{-1} of water) for a selected aerosol bin with the initial midpoint diameter of 85 nm for the Base and KeepSO4 model scenarios.

density of larger particles is due to their larger sulfate content, as governed by the polydisperse seed particle composition.

Figure 5 shows the simulated aerosol pH, calculated as the negative logarithm of H^+ activity coefficient multiplied by H^+ mole fraction in particle liquid water. H+ activity coefficient and its mole fraction within the inorganic core are both calculated in the MOSAIC model at each time step. The model reveals that aerosol acidity changes by more than 2 pH units from its initial value (pH = −3.43), as illustrated in Figure 5 for a selected size bin. The rapid change in aerosol acidity after a few minutes is consistent with the declining total inorganic sulfate species (SO_4^{2-} and HSO_4^-) resulting from conversion into OSs. It has been well demonstrated that the conversion of inorganic to organic sulfate is driven primarily by the IEPOX to inorganic sulfate ratio (IEPOX:$Sulf_{inorg}$), with IEPOX:Sul f_{inorg} > 10, leading to more rapid conversion of aqueous inorganic sulfate to organic components and a corresponding large increase in particle pH (lower acidity).[11,39] Measure ments in Riva et al. were conducted at an initial IEPOX:$Sulf_{inorg}$ of >20. Our simulations show that for these conditions ∼80% of inorganic sulfate is converted to organo sulfates resulting in a rapid decrease in aerosol acidity. Furthermore, OS formation also decreases aerosol hygro scopicity and diffusivity, thus limiting further IEPOX uptake.

Effect of Mass Accommodation Coefficient. Particle growth is found to be sensitive to the mass accommodation coefficient (α) of IEPOX, a quantity describing the interfacial limitations to gaseous uptake by seed particles. It is notable that changing α from 0.02, as applied in *Base* scenario, to 0.1, as applied in *HighAccom* scenario, can increase the growth in particle number mean diameter and suspended particle volume concentration by ∼8% and ∼15%, respectively (Figure 2). These results are expected, as larger values of α indicate increased gas uptake into the particle bulk. However, since α is less than unity (α = 1), there still exists some barrier to mass transfer, which could be either in the condensed phase or at the particle−vapor interface. Higher α improves the model performance of predicted aerosol growth (Table 1 and Figure 2), but the number size distribution tends to get narrower, and the peak is higher than observations (Figure 3). Changing the α value has no discernible effect on SOA composition as shown in Figure 4, with differences between the two scenarios being less than 3%.

Effect of Accounting for Molar Balance between Organic and Inorganic Sulfates. Most modeling studies do not account for sulfate balance in IEPOX OS formation.[46,47,62] In our simulations above we subtracted the molar concen tration of OS from inorganic sulfate at each time step, accounting for the conversion of inorganic sulfate to OS. To demonstrate the effect of this molar sulfate balance, we conducted a sensitivity study, wherein we turned off the removal of equimolar inorganic sulfate concentrations as OS forms (KeepSO4). This KeepSO4 scenario predicts a large increase in the particle number mean diameter and total volume growth, particularly after 40 min, and overpredicts observations by ∼45% and ∼85%, respectively, at the end of the experiment (Figure 2). The final mean particle diameter and total volume concentration in this scenario are 189.6 nm and 79.8 μm^3 cm^{-3}, respectively (Table 1). Compared to the base case, the predicted OS contribution to IEPOX SOA within KeepSO4 decreases by ∼12% although it still dominates the SOA composition (Figure 4). On the other hand, the contribution of tetrols and its oligomers to IEPOX SOA increases by 6% compared to the base case.

The major change in KeepSO4 compared to the base scenario is reflected in changes of particle acidity. While in the base case pH increases by more than 2 pH units due to consumption of inorganic sulfate during OS formation, the KeepSO4 formulation predicts a constant pH throughout the experiment as inorganic sulfate content per particle liquid water does not change (Figure 5).

■ CONCLUSIONS

We derive unique insights into IEPOX SOA processes by integrating our newly developed IEPOX SOA formulations in a box model and unique single particle measurements of IEPOX derived SOA formation. While previous studies have either focused on measuring bulk kinetics, or short time scale

(~seconds) flow tube measurements of gas phase IEPOX loss during IEPOX SOA formation, we find that single particle measurements within a chamber at longer time scales (~hours) and modeling of IEPOX SOA processes provide key and valuable additional insights. We evaluate several measured parameters of IEPOX SOA simultaneously: particle size evolution, chemical composition, density, and volatility.

We find that including diffusion limitations in IEPOX SOA organic phase and imposing an organic and inorganic sulfate molar balance are critical to explaining measured IEPOX SOA multiphase chemistry and kinetics. Our model can simulate IEPOX SOA formation leading to the growth of particle mean diameter and total suspended particle volume concentrations. The model also well reproduces the observed shape of the number size distributions although it underpredicts observed aerosol mean diameter by 7% and total suspended particle volume by ~24% at the end of the experiment. However, the model overpredicts the initial growth (at t = 10 min) likely because the model was initialized "instantaneously" with gaseous IEPOX of 500 ppb and the SMPS measured seed aerosol size distribution before the IEPOX injection, whereas in the experiment, it took a few minutes to inject IEPOX into the 1 m^3 chamber and mix it with the ABS seed particles. The model reproduces the observed uniform aerosol density across particle sizes with a bias of less than 12%.

The present work supports the application of IEPOX reactive uptake as an acidity dependent SOA formation process in models and the potential impact of IEPOX derived SOA coatings to inhibit further SOA formation. It should be noted that the model is sensitive to the mass accommodation coefficient of IEPOX, wherein a higher value of this parameter would lead to improved particle growth evolution, but the aerosol size distribution tends to be narrower, and the peak is taller than the observed data. The result entails that this parameter needs to be well constrained for accurate modeling of IEPOX SOA. Our sensitivity study also reveals that the predicted evolution of aerosol size and volume are over estimated when inorganic sulfate is not removed during OS formation, thus highlighting the importance of accounting for the consumption of inorganic sulfate during the production of particulate OSs.

■ ASSOCIATED CONTENT

● Supporting Information

The Supporting Information is available free of charge at https://pubs.acs.org/doi/10.1021/acsearthspacechem.1c00303.

> Additional information on the schematic of the chamber experimental setup, particle phase reaction rate constant (k_{aq}), selecting $H_{org}D_{org}$ and H_{aq} parameters, aerosol wall loss, comparison between simulated results and ob servations for the size distribution of final aerosol density, and references (PDF)

■ AUTHOR INFORMATION

Corresponding Author

Manish Shrivastava − *Pacific Northwest National Laboratory, Richland, Washington 99352, United States;* orcid.org/0000 0002 9053 2400; Email: manishkumar.shrivastava@pnnl.gov

Authors

Mega Octaviani − *Pacific Northwest National Laboratory, Richland, Washington 99352, United States;* Present Address: Institute of Meteorology and Climate Research, Department of Troposphere Research, Karlsruhe Institute of Technology, Karlsruhe 76021, Germany

Rahul A. Zaveri − *Pacific Northwest National Laboratory, Richland, Washington 99352, United States;* orcid.org/0000 0001 9874 8807

Alla Zelenyuk − *Pacific Northwest National Laboratory, Richland, Washington 99352, United States*

Yue Zhang − *Department of Atmospheric Sciences, Texas A&M University, College Station, Texas 77843, United States; Department of Environmental Sciences and Engineering, Gillings School of Global Public Health, University of North Carolina at Chapel Hill, Chapel Hill, North Carolina 27599, United States*

Quazi Z. Rasool − *Pacific Northwest National Laboratory, Richland, Washington 99352, United States;* orcid.org/0000 0001 6274 6236

David M. Bell − *Laboratory of Atmospheric Chemistry, Paul Scherrer Institute, Villigen 5232, Switzerland*

Matthieu Riva − *Université Lyon, Université Claude Bernard Lyon 1, CNRS, IRCELYON, 69626 Villeurbanne, France;* orcid.org/0000 0003 0054 4131

Marianne Glasius − *Department of Chemistry, Aarhus University, Aarhus C 8000, Denmark;* orcid.org/0000 0002 4404 6989

Jason D. Surratt − *Department of Environmental Sciences and Engineering, Gillings School of Global Public Health and Department of Chemistry, College of Arts and Sciences, University of North Carolina at Chapel Hill, Chapel Hill, North Carolina 27599, United States;* orcid.org/0000 0002 6833 1450

Complete contact information is available at: https://pubs.acs.org/10.1021/acsearthspacechem.1c00303

Author Contributions

M.S. designed and supervised the overall project. M.S. and M.O. implemented the IEPOX SOA box model developments with contributions from R.A.Z., A.Z., and Y.Z. M.O. performed box model simulations and created visualizations. M.O. and M.S. wrote the manuscript with contributions from all coauthors.

Notes

The authors declare no competing financial interest.

■ ACKNOWLEDGMENTS

This research was supported by the U.S. Department of Energy (DOE) Office of Science, Office of Biological and Environ mental Research. M.S., M.O., and Q.Z.R. were supported by the U.S. DOE, Office of Science, Office of Biological and Environmental Research through the Early Career Research Program. R.A.Z. and A.Z. were supported by the DOE's Atmospheric System Research Program. Pacific Northwest National Laboratory (PNNL) is operated for DOE by the Battelle Memorial Institute under contract No. DE A05 76RLO1830. M.R. and J.D.S. wish to thank the Camille and Henry Dreyfus Postdoctoral Fellowship Program in Environ mental Chemistry for their financial support. M.O. received partial support for this work through the Helmholtz Association's Initiative and Networking Fund (No. VH NG

1533). Y.Z. acknowledges the support from NSF Division of Atmospheric Geospace Sciences (AGS) Grant No. 2001027 and the National Institutes of Health (NIH) training Grant No. T32ES007018. The experimental studies used in this work were performed at and supported by EMSL, a DOE Office of Science User Facility sponsored by the Office of Biological and Environmental Research and located at Pacific Northwest National Laboratory. Computational resources were provided by the PNNL Institutional Computing facility and EMSL.

REFERENCES

(1) Guenther, A.; Karl, T.; Harley, P.; Wiedinmyer, C.; Palmer, P. I.; Geron, C. Estimates of global terrestrial isoprene emissions using MEGAN (Model of Emissions of Gases and Aerosols from Nature). *Atmos. Chem. Phys.* **2006**, *6* (11), 3181−3210.

(2) Atkinson, R. Gas phase tropospheric chemistry of volatile organic compounds: 1. Alkanes and alkenes. *J. Phys. Chem. Ref. Data* **1997**, *26* (2), 215−290.

(3) Carlton, A. G.; Wiedinmyer, C.; Kroll, J. H. A review of secondary organic aerosol (SOA) formation from isoprene. *Atmos. Chem. Phys.* **2009**, *9* (14), 4987−5005.

(4) Henze, D. K.; Seinfeld, J. H. Global secondary organic aerosol from isoprene oxidation. *Geophys. Res. Lett.* **2006**, *33* (9), No. 2006GL025976, DOI: 10.1029/2006GL025976.

(5) Shrivastava, M.; Cappa, C. D.; Fan, J.; Goldstein, A. H.; Guenther, A. B.; Jimenez, J. L.; Kuang, C.; Laskin, A.; Martin, S. T.; Ng, N. L.; Petaja, T.; Pierce, J. R.; Rasch, P. J.; Roldin, P.; Seinfeld, J. H.; Shilling, J.; Smith, J. N.; Thornton, J. A.; Volkamer, R.; Wang, J.; Worsnop, D. R.; Zaveri, R. A.; Zelenyuk, A.; Zhang, Q. Recent advances in understanding secondary organic aerosol: Implications for global climate forcing. *Rev. Geophys.* **2017**, *55* (2), 509−559.

(6) Claeys, M.; Graham, B.; Vas, G.; Wang, W.; Vermeylen, R.; Pashynska, V.; Cafmeyer, J.; Guyon, P.; Andreae, M. O.; Artaxo, P.; Maenhaut, W. Formation of secondary organic aerosols through photooxidation of isoprene. *Science* **2004**, *303* (5661), 1173−1176.

(7) Edney, E. O.; Kleindienst, T. E.; Jaoui, M.; Lewandowski, M.; Offenberg, J. H.; Wang, W.; Claeys, M. Formation of 2 methyl tetrols and 2 methylglyceric acid in secondary organic aerosol from laboratory irradiated isoprene/NOX/SO2/air mixtures and their detection in ambient PM2.5 samples collected in the eastern United States. *Atmos. Environ.* **2005**, *39* (29), 5281−5289.

(8) Surratt, J. D.; Murphy, S. M.; Kroll, J. H.; Ng, N. L.; Hildebrandt, L.; Sorooshian, A.; Szmigielski, R.; Vermeylen, R.; Maenhaut, W.; Claeys, M.; Flagan, R. C.; Seinfeld, J. H. Chemical composition of secondary organic aerosol formed from the photooxidation of isoprene. *J. Phys. Chem. A* **2006**, *110* (31), 9665−9690.

(9) Kroll, J. H.; Ng, N. L.; Murphy, S. M.; Flagan, R. C.; Seinfeld, J. H. Secondary organic aerosol formation from isoprene photo oxidation. *Environ. Sci. Technol.* **2006**, *40* (6), 1869−1877.

(10) Surratt, J. D.; Chan, A. W. H.; Eddingsaas, N. C.; Chan, M.; Loza, C. L.; Kwan, A. J.; Hersey, S. P.; Flagan, R. C.; Wennberg, P. O.; Seinfeld, J. H. Reactive intermediates revealed in secondary organic aerosol formation from isoprene. *Proc. Natl. Acad. Sci. U. S. A.* **2010**, *107* (15), 6640−6645.

(11) Riva, M.; Chen, Y.; Zhang, Y.; Lei, Z.; Olson, N. E.; Boyer, H. C.; Narayan, S.; Yee, L. D.; Green, H. S.; Cui, T.; Zhang, Z.; Baumann, K.; Fort, M.; Edgerton, E.; Budisulistiorini, S. H.; Rose, C. A.; Ribeiro, I. O.; e Oliveira, R. L.; dos Santos, E. O.; Machado, C. M. D.; Szopa, S.; Zhao, Y.; Alves, E. G.; de Sá, S. S.; Hu, W.; Knipping, E. M.; Shaw, S. L.; Duvoisin Junior, S.; de Souza, R. A. F.; Palm, B. B.; Jimenez, J. L.; Glasius, M.; Goldstein, A. H.; Pye, H. O. T.; Gold, A.; Turpin, B. J.; Vizuete, W.; Martin, S. T.; Thornton, J. A.; Dutcher, C. S.; Ault, A. P.; Surratt, J. D. Increasing isoprene epoxydiol to inorganic sulfate aerosol ratio results in extensive conversion of inorganic sulfate to organosulfur forms: Implications for aerosol physicochemical properties. *Environ. Sci. Technol.* **2019**, *53* (15), 8682−8694.

(12) Chen, Y.; Zhang, Y.; Lambe, A. T.; Xu, R.; Lei, Z.; Olson, N. E.; Zhang, Z.; Szalkowski, T.; Cui, T.; Vizuete, W.; Gold, A.; Turpin, B. J.; Ault, A. P.; Chan, M. N.; Surratt, J. D. Heterogeneous Hydroxyl Radical Oxidation of Isoprene Epoxydiol Derived Methyltetrol Sulfates: Plausible Formation Mechanisms of Previously Unexplained Organosulfates in Ambient Fine Aerosols. *Environ. Sci. Technol. Lett.* **2020**, *7* (7), 460−468.

(13) Froyd, K. D.; Murphy, S. M.; Murphy, D. M.; de Gouw, J. A.; Eddingsaas, N. C.; Wennberg, P. O. Contribution of isoprene derived organosulfates to free tropospheric aerosol mass. *Proc. Natl. Acad. Sci. U. S. A.* **2010**, *107* (50), 21360−21365.

(14) Surratt, J. D.; Gómez González, Y.; Chan, A. W. H.; Vermeylen, R.; Shahgholi, M.; Kleindienst, T. E.; Edney, E. O.; Offenberg, J. H.; Lewandowski, M.; Jaoui, M.; Maenhaut, W.; Claeys, M.; Flagan, R. C.; Seinfeld, J. H. Organosulfate formation in biogenic secondary organic aerosol. *J. Phys. Chem. A* **2008**, *112* (36), 8345−8378.

(15) Wang, W.; Kourtchev, I.; Graham, B.; Cafmeyer, J.; Maenhaut, W.; Claeys, M. Characterization of oxygenated derivatives of isoprene related to 2 methyltetrols in Amazonian aerosols using trimethylsily lation and gas chromatography/ion trap mass spectrometry. *Rapid Commun. Mass Spectrom.* **2005**, *19* (10), 1343−1351.

(16) Chan, M. N.; Surratt, J. D.; Claeys, M.; Edgerton, E. S.; Tanner, R. L.; Shaw, S. L.; Zheng, M.; Knipping, E. M.; Eddingsaas, N. C.; Wennberg, P. O.; Seinfeld, J. H. Characterization and quantification of isoprene derived epoxydiols in ambient aerosol in the southeastern United States. *Environ. Sci. Technol.* **2010**, *44* (12), 4590−4596.

(17) Hallquist, M.; Wenger, J. C.; Baltensperger, U.; Rudich, Y.; Simpson, D.; Claeys, M.; Dommen, J.; Donahue, N. M.; George, C.; Goldstein, A. H.; Hamilton, J. F.; Herrmann, H.; Hoffmann, T.; Iinuma, Y.; Jang, M.; Jenkin, M. E.; Jimenez, J. L.; Kiendler Scharr, A.; Maenhaut, W.; McFiggans, G.; Mentel, T. F.; Monod, A.; Prévôt, A. S. H.; Seinfeld, J. H.; Surratt, J. D.; Szmigielski, R.; Wildt, J. The formation, properties and impact of secondary organic aerosol: current and emerging issues. *Atmos. Chem. Phys.* **2009**, *9* (14), 5155−5236.

(18) Heald, C. L.; Henze, D. K.; Horowitz, L. W.; Feddema, J.; Lamarque, J. F.; Guenther, A.; Hess, P. G.; Vitt, F.; Seinfeld, J. H.; Goldstein, A. H.; Fung, I. Predicted change in global secondary organic aerosol concentrations in response to future climate, emissions, and land use change. *J. Geophys. Res.: Atmos.* **2008**, *113* (D5), No. 2007JD009092.

(19) Bates, K. H.; Crounse, J. D.; St. Clair, J. M.; Bennett, N. B.; Nguyen, T. B.; Seinfeld, J. H.; Stoltz, B. M.; Wennberg, P. O. Gas phase production and loss of isoprene epoxydiols. *J. Phys. Chem. A* **2014**, *118* (7), 1237−1246.

(20) Paulot, F.; Crounse, J. D.; Kjaergaard, H. G.; Kürten, A.; St. Clair, J. M.; Seinfeld, J. H.; Wennberg, P. O. Unexpected epoxide formation in the gas phase photooxidation of isoprene. *Science* **2009**, *325* (5941), 730.

(21) Cole Filipiak, N. C.; O'Connor, A. E.; Elrod, M. J. Kinetics of the hydrolysis of atmospherically relevant isoprene derived hydroxy epoxides. *Environ. Sci. Technol.* **2010**, *44* (17), 6718−6723.

(22) Lin, Y. H.; Zhang, Z.; Docherty, K. S.; Zhang, H.; Budisulistiorini, S. H.; Rubitschun, C. L.; Shaw, S. L.; Knipping, E. M.; Edgerton, E. S.; Kleindienst, T. E.; Gold, A.; Surratt, J. D. Isoprene epoxydiols as precursors to secondary organic aerosol formation: acid catalyzed reactive uptake studies with authentic compounds. *Environ. Sci. Technol.* **2012**, *46* (1), 250−258.

(23) Surratt, J. D.; Lewandowski, M.; Offenberg, J. H.; Jaoui, M.; Kleindienst, T. E.; Edney, E. O.; Seinfeld, J. H. Effect of acidity on secondary organic aerosol formation from isoprene. *Environ. Sci. Technol.* **2007**, *41* (15), 5363−5369.

(24) Eddingsaas, N. C.; VanderVelde, D. G.; Wennberg, P. O. Kinetics and products of the acid catalyzed ring opening of atmospherically relevant butyl epoxy alcohols. *J. Phys. Chem. A* **2010**, *114* (31), 8106−8113.

(25) Lin, Y. H.; Budisulistiorini, S. H.; Chu, K.; Siejack, R. A.; Zhang, H.; Riva, M.; Zhang, Z.; Gold, A.; Kautzman, K. E.; Surratt, J. D. Light absorbing oligomer formation in secondary organic aerosol

from reactive uptake of isoprene epoxydiols. *Environ. Sci. Technol.* **2014**, *48* (20), 12012−12021.
(26) Budisulistiorini, S. H.; Canagaratna, M. R.; Croteau, P. L.; Marth, W. J.; Baumann, K.; Edgerton, E. S.; Shaw, S. L.; Knipping, E. M.; Worsnop, D. R.; Jayne, J. T.; Gold, A.; Surratt, J. D. Real time continuous characterization of secondary organic aerosol derived from isoprene epoxydiols in downtown Atlanta, Georgia, using the aerodyne aerosol chemical speciation monitor. *Environ. Sci. Technol.* **2013**, *47* (11), 5686−5694.
(27) Lin, Y. H.; Knipping, E. M.; Edgerton, E. S.; Shaw, S. L.; Surratt, J. D. Investigating the influences of SO2 and NH3 levels on isoprene derived secondary organic aerosol formation using condi tional sampling approaches. *Atmos. Chem. Phys.* **2013**, *13* (16), 8457−8470.
(28) Budisulistiorini, S. H.; Li, X.; Bairai, S. T.; Renfro, J.; Liu, Y.; Liu, Y. J.; McKinney, K. A.; Martin, S. T.; McNeill, V. F.; Pye, H. O. T.; Nenes, A.; Neff, M. E.; Stone, E. A.; Mueller, S.; Knote, C.; Shaw, S. L.; Zhang, Z.; Gold, A.; Surratt, J. D. Examining the effects of anthropogenic emissions on isoprene derived secondary organic aerosol formation during the 2013 Southern Oxidant and Aerosol Study (SOAS) at the Look Rock, Tennessee, ground site. *Atmos. Chem. Phys.* **2015**, *15* (15), 8871−8888.
(29) Chen, Q.; Farmer, D. K.; Rizzo, L. V.; Pauliquevis, T.; Kuwata, M.; Karl, T. G.; Guenther, A.; Allan, J. D.; Coe, H.; Andreae, M. O.; Pöschl, U.; Jimenez, J. L.; Artaxo, P.; Martin, S. T. Submicron particle mass concentrations and sources in the Amazonian wet season (AMAZE 08). *Atmos. Chem. Phys.* **2015**, *15* (7), 3687−3701.
(30) Xu, L.; Guo, H.; Boyd, C. M.; Klein, M.; Bougiatioti, A.; Cerully, K. M.; Hite, J. R.; Isaacman VanWertz, G.; Kreisberg, N. M.; Knote, C.; Olson, K.; Koss, A.; Goldstein, A. H.; Hering, S. V.; De Gouw, J.; Baumann, K.; Lee, S. H.; Nenes, A.; Weber, R. J.; Ng, N. L. Effects of anthropogenic emissions on aerosol formation from isoprene and monoterpenes in the southeastern United States. *Proc. Natl. Acad. Sci. U. S. A.* **2015**, *112* (1), 37−42.
(31) Rattanavaraha, W.; Chu, K.; Budisulistiorini, S. H.; Riva, M.; Lin, Y. H.; Edgerton, E. S.; Baumann, K.; Shaw, S. L.; Guo, H.; King, L.; Weber, R. J.; Neff, M. E.; Stone, E. A.; Offenberg, J. H.; Zhang, Z.; Gold, A.; Surratt, J. D. Assessing the impact of anthropogenic pollution on isoprene derived secondary organic aerosol formation in PM2.5 collected from the Birmingham, Alabama, ground site during the 2013 Southern Oxidant and Aerosol Study. *Atmos. Chem. Phys.* **2016**, *16* (8), 4897−4914.
(32) Gaston, C. J.; Riedel, T. P.; Zhang, Z.; Gold, A.; Surratt, J. D.; Thornton, J. A. Reactive uptake of an isoprene derived epoxydiol to submicron aerosol particles. *Environ. Sci. Technol.* **2014**, *48* (19), 11178−11186.
(33) Riedel, T. P.; Lin, Y. H.; Budisulistiorini, S. H.; Gaston, C. J.; Thornton, J. A.; Zhang, Z.; Vizuete, W.; Gold, A.; Surratt, J. D. Heterogeneous reactions of isoprene derived epoxides: reaction probabilities and molar secondary organic aerosol yield estimates. *Environ. Sci. Technol. Lett.* **2015**, *2* (2), 38−42.
(34) Zhang, Y.; Chen, Y.; Lambe, A. T.; Olson, N. E.; Lei, Z.; Craig, R. L.; Zhang, Z.; Gold, A.; Onasch, T. B.; Jayne, J. T.; Worsnop, D. R.; Gaston, C. J.; Thornton, J. A.; Vizuete, W.; Ault, A. P.; Surratt, J. D. Effect of the aerosol phase state on secondary organic aerosol formation from the reactive uptake of isoprene derived epoxydiols (IEPOX). *Environ. Sci. Technol. Lett.* **2018**, *5* (3), 167−174.
(35) Riva, M.; Bell, D. M.; Hansen, A. M. K.; Drozd, G. T.; Zhang, Z.; Gold, A.; Imre, D.; Surratt, J. D.; Glasius, M.; Zelenyuk, A. Effect of organic coatings, humidity and aerosol acidity on multiphase chemistry of isoprene epoxydiols. *Environ. Sci. Technol.* **2016**, *50* (11), 5580−5588.
(36) Bertram, A. K.; Martin, S. T.; Hanna, S. J.; Smith, M. L.; Bodsworth, A.; Chen, Q.; Kuwata, M.; Liu, A.; You, Y.; Zorn, S. R. Predicting the relative humidities of liquid liquid phase separation, efflorescence, and deliquescence of mixed particles of ammonium sulfate, organic material, and water using the organic to sulfate mass ratio of the particle and the oxygen to carbon elemental ratio of the organic component. *Atmos. Chem. Phys.* **2011**, *11* (21), 10995−11006.
(37) Schmedding, R.; Rasool, Q. Z.; Zhang, Y.; Pye, H. O. T.; Zhang, H.; Chen, Y.; Surratt, J. D.; Lopez Hilfiker, F. D.; Thornton, J. A.; Goldstein, A. H.; Vizuete, W. Predicting secondary organic aerosol phase state and viscosity and its effect on multiphase chemistry in a regional scale air quality model. *Atmos. Chem. Phys.* **2020**, *20* (13), 8201−8225.
(38) Ciobanu, V. G.; Marcolli, C.; Krieger, U. K.; Weers, U.; Peter, T. Liquid−liquid phase separation in mixed organic/inorganic aerosol particles. *J. Phys. Chem. A* **2009**, *113* (41), 10966−10978.
(39) Zhang, Y.; Chen, Y.; Lei, Z.; Olson, N.; Riva, M.; Koss, A. R.; Zhang, Z.; Gold, A.; Jayne, J. T.; Worsnop, D. R.; Onasch, T. B.; Kroll, J. H.; Turpin, B. J.; Ault, A. P.; Surratt, J. D. Joint impacts of acidity and viscosity on the formation of secondary organic aerosol from isoprene epoxydiols (IEPOX) in phase separated particles. *ACS Earth Space Chem.* **2019**, *3*, 2646.
(40) Zhang, Y.; Nichman, L.; Spencer, P.; Jung, J. I.; Lee, A.; Heffernan, B. K.; Gold, A.; Zhang, Z.; Chen, Y.; Canagaratna, M. R.; Jayne, J. T.; Worsnop, D. R.; Onasch, T. B.; Surratt, J. D.; Chandler, D.; Davidovits, P.; Kolb, C. E. The cooling rate and volatility dependent glass forming properties of organic aerosols measured by broadband dielectric spectroscopy. *Environ. Sci. Technol.* **2019**, *53*, 12366.
(41) Anttila, T.; Kiendler Scharr, A.; Tillmann, R.; Mentel, T. F. On the reactive uptake of gaseous compounds by organic coated aqueous aerosols: theoretical analysis and application to the heterogeneous hydrolysis of N2O5. *J. Phys. Chem. A* **2006**, *110* (35), 10435−10443.
(42) Gaston, C. J.; Thornton, J. A.; Ng, N. L. Reactive uptake of N2O5 to internally mixed inorganic and organic particles: The role of organic carbon oxidation state and inferred organic phase separations. *Atmos. Chem. Phys.* **2014**, *14* (11), 5693−5707.
(43) Piletic, I. R.; Edney, E. O.; Bartolotti, L. J. A computational study of acid catalyzed aerosol reactions of atmospherically relevant epoxides. *Phys. Chem. Chem. Phys.* **2013**, *15* (41), 18065−18076.
(44) Nguyen, T. B.; Coggon, M. M.; Bates, K. H.; Zhang, X.; Schwantes, R. H.; Schilling, K. A.; Loza, C. L.; Flagan, R. C.; Wennberg, P. O.; Seinfeld, J. H. Organic aerosol formation from the reactive uptake of isoprene epoxydiols (IEPOX) onto non acidified inorganic seeds. *Atmos. Chem. Phys.* **2014**, *14* (7), 3497−3510.
(45) Riedel, T. P.; Lin, Y. H.; Zhang, Z.; Chu, K.; Thornton, J. A.; Vizuete, W.; Gold, A.; Surratt, J. D. Constraining condensed phase formation kinetics of secondary organic aerosol components from isoprene epoxydiols. *Atmos. Chem. Phys.* **2016**, *16* (3), 1245−1254.
(46) Budisulistiorini, S. H.; Nenes, A.; Carlton, A. G.; Surratt, J. D.; McNeill, V. F.; Pye, H. O. T. Simulating aqueous phase isoprene epoxydiol (IEPOX) secondary organic aerosol production during the 2013 Southern Oxidant and Aerosol Study (SOAS). *Environ. Sci. Technol.* **2017**, *51* (9), 5026−5034.
(47) Pye, H. O. T.; Pinder, R. W.; Piletic, I. R.; Xie, Y.; Capps, S. L.; Lin, Y. H.; Surratt, J. D.; Zhang, Z.; Gold, A.; Luecken, D. J.; Hutzell, W. T.; Jaoui, M.; Offenberg, J. H.; Kleindienst, T. E.; Lewandowski, M.; Edney, E. O. Epoxide pathways improve model predictions of isoprene markers and reveal key role of acidity in aerosol formation. *Environ. Sci. Technol.* **2013**, *47* (19), 11056−11064.
(48) Marais, E. A.; Jacob, D. J.; Jimenez, J. L.; Campuzano Jost, P.; Day, D. A.; Hu, W.; Krechmer, J.; Zhu, L.; Kim, P. S.; Miller, C. C.; Fisher, J. A.; Travis, K.; Yu, K.; Hanisco, T. F.; Wolfe, G. M.; Arkinson, H. L.; Pye, H. O. T.; Froyd, K. D.; Liao, J.; McNeill, V. F. Aqueous phase mechanism for secondary organic aerosol formation from isoprene: application to the southeast United States and co benefit of SO2 emission controls. *Atmos. Chem. Phys.* **2016**, *16* (3), 1603−1618.
(49) Zaveri, R. A.; Easter, R. C.; Fast, J. D.; Peters, L. K. Model for Simulating Aerosol Interactions and Chemistry (MOSAIC). *J. Geophys. Res.* **2008**, *113* (D13), No. 2007JD008782, DOI: 10.1029/2007JD008782.
(50) Shrivastava, M.; Fast, J.; Easter, R.; Gustafson, W. I., Jr; Zaveri, R. A.; Jimenez, J. L.; Saide, P.; Hodzic, A. Modeling organic aerosols

in a megacity: comparison of simple and complex representations of the volatility basis set approach. *Atmos. Chem. Phys.* **2011**, *11* (13), 6639−6662.
(51) Shrivastava, M.; Andreae, M. O.; Artaxo, P.; Barbosa, H. M. J.; Berg, L. K.; Brito, J.; Ching, J.; Easter, R. C.; Fan, J.; Fast, J. D.; Feng, Z.; Fuentes, J. D.; Glasius, M.; Goldstein, A. H.; Alves, E. G.; Gomes, H.; Gu, D.; Guenther, A.; Jathar, S. H.; Kim, S.; Liu, Y.; Lou, S.; Martin, S. T.; McNeill, V. F.; Medeiros, A.; de Sá, S. S.; Shilling, J. E.; Springston, S. R.; Souza, R. A. F.; Thornton, J. A.; Isaacman VanWertz, G.; Yee, L. D.; Ynoue, R.; Zaveri, R. A.; Zelenyuk, A.; Zhao, C. Urban pollution greatly enhances formation of natural aerosols over the Amazon rainforest. *Nat. Commun.* **2019**, *10* (1), 1046.
(52) Zaveri, R. A.; Easter, R. C.; Singh, B.; Wang, H.; Lu, Z.; Tilmes, S.; Emmons, L. K.; Vitt, F.; Zhang, R.; Liu, X.; Ghan, S. J.; Rasch, P. J. Development and Evaluation of Chemistry Aerosol Climate Model CAM5 Chem MAM7 MOSAIC: Global Atmospheric Distribution and Radiative Effects of Nitrate Aerosol. *J. Adv. Model. Earth Syst.* **2021**, *13* (4), e2020MS002346.
(53) Zaveri, R. A.; Easter, R. C.; Shilling, J. E.; Seinfeld, J. H. Modeling kinetic partitioning of secondary organic aerosol and size distribution dynamics: representing effects of volatility, phase state, and particle phase reaction. *Atmos. Chem. Phys.* **2014**, *14* (10), 5153−5181.
(54) Zhang, Z.; Lin, Y. H.; Zhang, H.; Surratt, J. D.; Ball, L. M.; Gold, A. Technical Note: Synthesis of isoprene atmospheric oxidation products: isomeric epoxydiols and the rearrangement products cis and trans 3 methyl 3,4 dihydroxytetrahydrofuran. *Atmos. Chem. Phys.* **2012**, *12* (18), 8529−8535.
(55) Zelenyuk, A.; Imre, D.; Wilson, J.; Zhang, Z.; Wang, J.; Mueller, K. Airborne single particle mass spectrometers (SPLAT II & miniSPLAT) and new software for data visualization and analysis in a geo spatial context. *J. Am. Soc. Mass Spectrom.* **2015**, *26* (2), 257−270.
(56) Zelenyuk, A.; Cai, Y.; Chieffo, L.; Imre, D. High Precision Density Measurements of Single Particles: The Density of Metastable Phases. *Aerosol Sci. Technol.* **2005**, *39* (10), 972−986.
(57) McNeill, V. F.; Woo, J. L.; Kim, D. D.; Schwier, A. N.; Wannell, N. J.; Sumner, A. J.; Barakat, J. M. Aqueous phase secondary organic aerosol and organosulfate formation in atmospheric aerosols: a modeling study. *Environ. Sci. Technol.* **2012**, *46* (15), 8075−8081.
(58) Pye, H. O. T.; Murphy, B. N.; Xu, L.; Ng, N. L.; Carlton, A. G.; Guo, H.; Weber, R.; Vasilakos, P.; Appel, K. W.; Budisulistiorini, S. H.; Surratt, J. D.; Nenes, A.; Hu, W.; Jimenez, J. L.; Isaacman VanWertz, G.; Misztal, P. K.; Goldstein, A. H. On the implications of aerosol liquid water and phase separation for organic aerosol mass. *Atmos. Chem. Phys.* **2017**, *17* (1), 343−369.
(59) Woo, J. L.; McNeill, V. F. simpleGAMMA v1.0 − a reduced model of secondary organic aerosol formation in the aqueous aerosol phase (aaSOA). *Geosci. Model Dev.* **2015**, *8* (6), 1821−1829.
(60) Cui, T.; Zeng, Z.; dos Santos, E. O.; Zhang, Z.; Chen, Y.; Zhang, Y.; Rose, C. A.; Budisulistiorini, S. H.; Collins, L. B.; Bodnar, W. M.; de Souza, R. A. F.; Martin, S. T.; Machado, C. M. D.; Turpin, B. J.; Gold, A.; Ault, A. P.; Surratt, J. D. Development of a hydrophilic interaction liquid chromatography (HILIC) method for the chemical characterization of water soluble isoprene epoxydiol (IEPOX) derived secondary organic aerosol. Environ. *Sci.: Processes Impacts* **2018**, *20* (11), 1524−1536.
(61) D'Ambro, E. L.; Schobesberger, S.; Gaston, C. J.; Lopez Hilfiker, F. D.; Lee, B. H.; Liu, J.; Zelenyuk, A.; Bell, D.; Cappa, C. D.; Helgestad, T.; Li, Z.; Guenther, A.; Wang, J.; Wise, M.; Caylor, R.; Surratt, J. D.; Riedel, T.; Hyttinen, N.; Salo, V. T.; Hasan, G.; Kurtén, T.; Shilling, J. E.; Thornton, J. A. Chamber based insights into the factors controlling epoxydiol (IEPOX) secondary organic aerosol (SOA) yield, composition, and volatility. *Atmos. Chem. Phys.* **2019**, *19* (17), 11253−11265.
(62) Schmedding, R.; Ma, M.; Zhang, Y.; Farrell, S.; Pye, H. O. T.; Chen, Y.; Wang, C. t.; Rasool, Q. Z.; Budisulistiorini, S. H.; Ault, A. P.; Surratt, J. D.; Vizuete, W. α Pinene Derived organic coatings on acidic sulfate aerosol impacts secondary organic aerosol formation from isoprene in a box model. *Atmos. Environ.* **2019**, *213*, 456−462.